GaInAsP/InP quantum wire lasers

著者	Arai Shigehisa, Maruyama Takeo
journal or publication title	IEEE Journal on Selected Topics in Quantum Electronics
volume	15
number	3
page range	731-742
year	2009-05-01
URL	http://hdl.handle.net/2297/19579

doi: 10.1109/JSTQE.2008.2010872

GaInAsP/InP Quantum Wire Lasers

Shigehisa Arai, *Senior Member, IEEE*, and Takeo Maruyama, *Member, IEEE*

(Invited Paper)

***Abstract*—Present status of GaInAsP/InP long-wavelength quantum wire lasers, fabricated by a method using electron beam exposure, dry etching, and two-step organometallic vapor-phase epitaxy, is described from aspects of low-damage interface formation and size uniformity of quantum wire structures. Even though superior lasing properties attributed to sharper gain spectrum over that of quantum well structure have not been realized yet, polarization anisotropic feature of the quantum wire structure and formation of good interfaces by this fabrication method were confirmed. Single-wavelength lasers consisting of quantum wire structure as the active and/or the passive regions have been realized as possible candidates for future integrated photonics.**

***Index Terms*—Distributed Bragg reflector (DBR) laser, distributed feedback (DFB) laser, distributed reflector (DR) laser, GaInAsP/InP, low-dimensional quantum well (QW) structure, polarization anisotropy, quantum wire laser.**

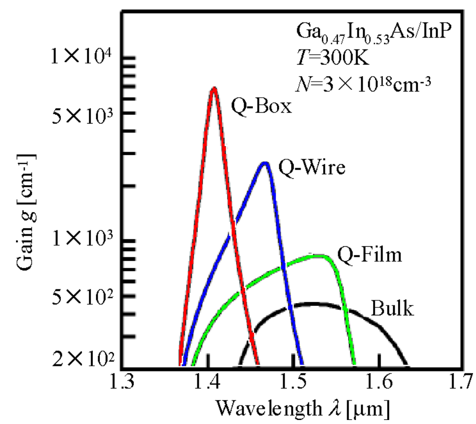

Fig. 1. Theoretical optical gain spectra of low-dimensional quantum structures by Asada *et al*. [6].

I. INTRODUCTION

SEMICONDUCTOR lasers are one of most successful photonic devices, benefitting from the quantum size effect, since their operation characteristics have been markedly improved by the introduction of lattice-matched (LM) [1] and strained [2]–[4] quantum well (QW) structures based on developments in epitaxial growth technologies enabling the realization of high-quality QW structures with precisely controlled thickness and composition. A further improvement in semiconductor laser performance is expected with the introduction of quantum confinement in more than one dimension. In low-dimensional QW structures, such as quantum wire (Q-wire) and quantum box (Q-box or Q-dot) structures, carriers are more strongly confined than in quantum film (Q-film) due to the further modification of band structures and density of states (DOSs) distributions [5].

Owing to the strong confinement of carriers into low-dimensional QW structures with sharper DOS features, higher optical gain and a narrower gain spectrum are obtained at the same injection current density and intraband relaxation time (0.1 ps). In other words, a higher differential gain can be obtained. Fig. 1 shows the calculated gain spectra of different quantized dimensions in the case of LM GaInAs/InP under the same injection carrier density [6]. Not only the sharpness of the gain spectrum but also its symmetric shape of lower dimensional structures was found to be very promising for narrow spectral chirp under a high-speed direct modulation and a narrow-linewidth operation due to reduced linewidth enhancement factor [7], [8]. Therefore, the threshold current, differential quantum efficiency, and linewidth of Q-wire and Q-box lasers have been expected to be superior to those of Q-film lasers [9]. Further improvements by a combination of strain and low-dimensional QW structures have also been expected [10].

The DOS distributions of Q-wire and Q-box structures are sharper than those of Q-films, but these sharp features are inferior owing to the size distributions of Q-wire and Q-box structures, leading to inhomogeneous broadening of the energy spectrum or spectral linewidth [11], [12]. The broadening significantly reduces the impact of the modified DOS, resulting in inferior optical gain and lasing properties.

In this paper, we would like to review fabrication methods and lasing performance of long-wavelength Q-wire lasers consisting of GaInAsP/InP system. Various fabrication methods and related accomplishments are reviewed in Section II, and theoretical investigations of gain and its polarization anisotropy are given in Section III. After explaining the fabrication method using an electron beam lithography (EBL) followed by low-damage dry etching and regrowth in Section IV, lasing properties of GaInAsP/InP long-wavelength Q-wire lasers, including polarization anisotropy of gain spectra measured in Fabry–Perot cavity lasers and low-threshold lasers by adopting distributed Bragg reflector (DBR) and distributed feedback (DFB) structures will be given in Section V.

Manuscript received November 3, 2008; revised; accepted November 25, 2008. First published; current version published. This work was supported in part by the Core Research for Evolutional Science Technology (CREST), Japan Science and Technology Agency, and by the Grants-in-Aid for Scientific Research from the Ministry of Education, Culture, Sports, Science and Technology, Japan.

S. Arai is with the Quantum Nanoelectronics Research Center, Tokyo Institute of Technology, Tokyo 152-8552, Japan (e-mail: arai@pe.titech.ac.jp).

T. Maruyama is with the School of Electrical and Computer Engineering, Kanazawa University, Ishikawa 920-1192, Japan (e-mail: maruyama@ec.t.kanazawa-u.ac.jp).

Color versions of one or more of the figures in this paper are available online at http://ieeexplore.ieee.org.

Digital Object Identifier 10.1109/JSTQE.2008.2010872

II. Fabrication Methods

A. Various Fabrication Techniques of Q-Wire Structures

To realize the high-performance operation of optical and/or electrical devices with low-dimensional quantum structures, a low-damage technology for the fabrication of ultrafine structures with good size uniformity is required, and various fabrication methods have been studied. The first attempt to fabricate GaAs Q-wire structures was carried out in 1982 by combining the growth of a QW structure followed by conventional lithography and a burial of the growth layer [13]. Similar technologies have also been investigated, including EB direct lithography and wet chemical etching [14], and dry etching [15], [16] followed by embedding growth [17], [18] for GaInAsP/InP, AlGaAs/GaAs [19], GaInAs/GaAs [20], [21] and $Si/Si_{1-x}Ge_x$ [22] systems. Other similar techniques including electrochemical anodization [23] and impact lithography [24] have also been attempted.

For GaAs/Al(In)GaAs systems, fractional layer growth on a tilted substrate [25] or multiatomic steps on a vicinal substrate [26]–[30] have been used to fabricate Q-wires, and QW structures have been grown on patterned substrates [31], [32] or on very fine V-shaped grooves (V-grooves) [33]–[35], since the oxidation of AlGaAs/GaAs is much severer and the surface recombination velocity of this system is much faster compared with GaInAsP/InP systems. Furthermore, for GaInAsP/InP systems, selective growth on a patterned substrate [36] or on V-grooves [37] as well as fractional layer growth on a vicinal InP substrate [38] have also been carried out for applications to single-electron devices or optical devices. Concerning other selective growth methods, the fabrication of Q-wires has also been attempted on grooved sidewalls [39], on cleaved edges [40], giant step edges on vicinal (1 1 0) surfaces [41], and (1 1 1)B facets by glancing angle molecular beam epitaxy (MBE) [42].

The aforementioned fabrication methods are much more difficult than those used to grow conventional Q-film structures, because the realization of high-quality QW structures with precisely controlled thickness and compositions is attributed only to developments in epitaxial growth technology. However, since 1990s, a simple technology for fabricating Q-wire or Q-box (Q-dot) structures directly on a substrate, involving only a growth technique has been investigated actively by many research groups, i.e., these structures can be self-assembled by adjusting the growth conditions. The strain-induced lateral-layer ordering (SI-LO) of binary superlattices was used [43]–[45]. The SI self-organized (SI-SO) growth technique using the Stranski–Krastanow (SK) epitaxial growth mode has been investigated [46]. The various fabrication methods of Q-wire structures are summarized in Fig. 2.: 1) fractional (submonoatomic) layer growth on the step edge of a vicinal substrate [13], [47], [48]; 2) a combination of lithography, etching, and embedding growth [49]–[52]; 3) selective growth on a patterned substrate [53]–[55]; 4) SI-LO of binary superlattices [56]; 5) SI-SO growth [46]; and 6) cleaved edge overgrowth [40].

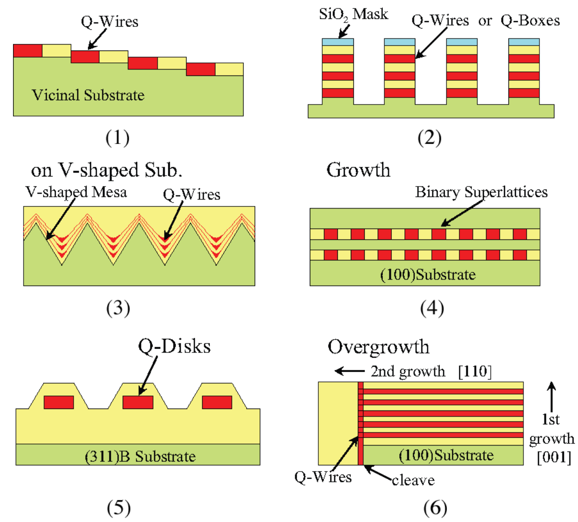

Fig. 2. Fabrication methods of Q-wire structures. (1) Titled Superlattices. (2) Lithography and Etching. (3) Selective Growth on V-shaped Sub. (4) Binary Superlattices Growth. (5) Self-organization. (6) Cleaved Edge Overgrowth.

We have investigated a fabrication method that combines EB lithography, etching, and two-step organometallic vapor-phase-epitaxial (OMVPE) growth, because this method has better position controllability and wider applications than other methods. These factors are important for achieving high-performance semiconductor lasers and various photonic devices with low-dimensional QW structures. It is also easy to apply an optional strained structure to Q-wire and Q-box lasers using this method, which is expected to render lasing properties superior to those of unstrained Q-wire and Q-box lasers [10]. Furthermore, this fabrication method is suitable for use in the production of DFB lasers [57]–[59]. In particular, a dry etching system should be applied to form high-density nanostructures with stacked multiple layers that are necessary for obtaining adequate optical confinement for a low-threshold-current operation.

B. Long-Wavelength Q-Wire and Q-Dot Lasers

The, so-called "long-wavelength" semiconductor lasers with wavelength of 1.3 and 1.55 μm are indispensable for optical fiber communication systems since the material dispersion of standard optical fiber is minimum at a wavelength of 1.3 μm and its loss is minimum at 1.55 μm. As explained in the previous section, various fabrication methods for Q-wire structures have been studied to realize high-performance semiconductor lasers. In 1993, a threshold current of as low as 16 mA and a threshold current density of 816 A/cm^2 were obtained under room temperature (RT) continuous-wave (CW) conditions for tensile-strained (TS) single-layered Q-wire lasers with 30–40-nm-wide and 70-nm-period wire active regions fabricated by EB lithography, wet etching, and two-step OMVPE growth [60], [61]. This method is the most direct approach for the fabrication of Q-wire and Q-box structures, and it is easy to control their size, density, and position. In particular, this fabrication method can control the lasing wavelength through the design of the initial QW and the size of the Q-wire or Q-box structure.

In 1996, single-layer Q-wire lasers were fabricated with a wire width of 20 nm in a period of 50 nm, which had a lower threshold current and a higher differential quantum efficiency than those of Q-film lasers at 200 K [62], [63]. On the other hand, not only wet chemical etching but also dry etching for the fabrication of stacked multiple-layered Q-wire and Q-box structures have been studied to obtain quantum structures with better uniformity so as to increase the optical confinement factor of the active region. In addition, for the fabrication of DFB lasers with wire-like active regions, dry etching yields a strong index-coupling coefficient because it can be used for deep etching. Although, there have been many reports on fabrication processes and photoluminescence (PL) or electroluminescence (EL) measurements for Q-wire and Q-box structures fabricated by dry etching [15], [16], [20], [51], [64]–[66], it seemed to be very difficult to use the dry etching method to obtain high-performance Q-wire and Q-box lasers due to the large amount of damage induced by fabrication. In 1995, Q-wire DFB lasers with wire widths of 140 nm down to 100 nm were reported [58]. These lasers were fabricated by electrocyclotron resonance-enhanced reactive ion-beam etching (ECR-RIBE) using a CCl_2F_2/Ar gas mixture [67] and wet chemical etching followed by OMVPE regrowth. In addition, by applying CH_4/H_2 reactive ion etching (RIE) to multiple QW (MQW) structures [68] and a much slower growth rate during the embedding growth of an InP layer than that used in conventional OMVPE growth [69], Q-wire lasers with lower threshold current density than that fabricated by wet chemical etching were obtained [59].

Using the SI-SO method, which is a self-assembled growth technology, a low-threshold current density of 16 A/cm^2 in 1.25-μm-wavelength InAs/GaInAs Q-dot lasers [70], a threshold current of 5.4 mA in 1.3-μm-wavelength GaInAs/GaAs Q-dot lasers [71], a threshold current of 17 mA and a submode suppression ratio (SMSR) of 55 dB in 1.3-μm-wavelength InAs/GaInAs Q-dot DFB lasers [72], and high-frequency operation [73] were demonstrated. To attain an emitting wavelength of 1.5 μm, InAs Q-dot lasers grown on (3 1 1)B-oriented InP substrate [74] and InAs Q-dash lasers on (1 0 0) InP substrate [75], [76] have been studied.

Furthermore, $Ga_xIn_{1-x}As/InP$ multiple-layered Q-wire lasers with an emitting wavelength of 1.69 μm at $T = 77$ K were fabricated by the SI-LO method [56], and GaInAs/InP single Q-wire lasers with an emitting wavelength of more than 1.3 μm at $T = 15$ K were fabricated by selective growth on a V-groove substrate [77].

III. Theoretical Analysis

A. Optical Gain

QW lasers with higher optical gain and reduced cavity loss can be achieved by reducing the volume of the active region, leading to low-threshold-current operation [4], [78], [79]. QW lasers also exhibit reduced temperature sensitivity, higher modulation bandwidths, and low-wavelength chirp operation. The material gain as a function of frequency is expressed as [80]

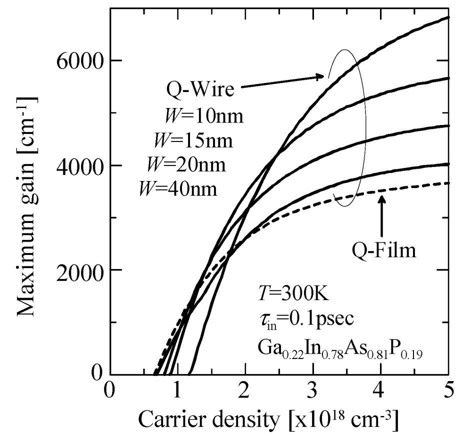

Fig. 3. Injection carrier density dependence of maximum gain for Q-wire structures with various wire widths.

$$g(\omega) = \frac{\omega}{n_r}\sqrt{\frac{\mu_0}{\varepsilon_0}}\int_{E_g}^{\infty}\langle \mathbf{R}_{cv}^2\rangle\, g_{cv}(E_{cv})\,\{f_c - f_v\} \times \frac{\hbar/\tau_{in}}{(E_{cv}-\hbar\omega)^2+(\hbar/\tau_{in})^2}\,dE_{cv} \qquad (1)$$

where the subscripts c and v denote the conduction and valence bands, respectively, ω is the angular frequency of the input light, n_r is the refractive index without the dispersion at the active region, $\langle R_{cv}\rangle^2$ is the transition matrix element of the dipole moment [81], [82], f_c and f_v are the Fermi functions for the conduction and valence bands, respectively, τ_{in} is the intraband relaxation time [83], and E_{cv} is the transition energy between the conduction and valence bands.

$g_{cv}(E_{cv})$, which is the DOSs in a Q-wire, is given by

$$g_{cv}(E_{cv}) = \left(\frac{2m_c^* m_v^*}{m_c^* + m_v^*}\right)^{1/2} \times \frac{1}{\pi\hbar W_x W_y}\bigg/ (E_{cv}-E_{cxy,l,m}-E_{vxy,l,m}-E_g)^{1/2} \qquad (2)$$

where m_c^* and m_v^* are the effective masses of an electron and hole, respectively, W_x and W_y are the width and thickness of the Q-wire, respectively, E_g is the band gap energy, and $E_{cxy,l,m}$ and $E_{vxy,l,m}$ are the quantized energy levels of the Q-wire in the conduction band and valence band, respectively.

Fig. 3 shows the injection carrier density dependence of maximum gain for a Q-wire structure with various wire widths (W). No difference between the Q-wire with $W = 40$ nm and the Q-film could be observed. Hence, to obtain improved optical gain properties due to the lateral confinement effect, Q-wire structures with a wire width of less than 20 nm should be realized.

B. Size Distribution of Optical Gain

In the previous section, the size distributions of Q-wire structures were not considered in the analysis. However, the

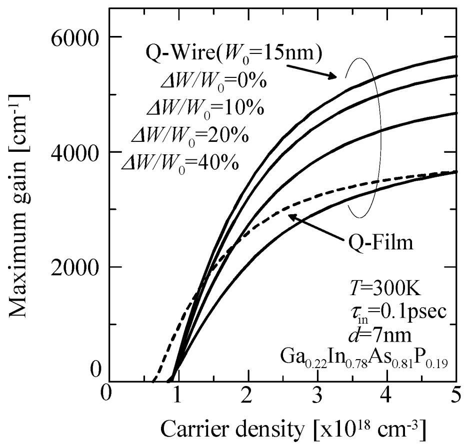

Fig. 4. Injection carrier density dependence of maximum gain for Q-wire structures with a wire width of 15 nm and a Q-film structure. The size distributions ($\Delta W/W_0$) are 0%, 10%, 20%, and 40%.

inhomogeneity of Q-wire structures due to the fabrication process has a strong effect on the lasing properties. Accordingly, the investigation of the permissible size distribution is very important for realizing applications of low-dimensional QW structures.

The injection carrier density dependence of maximum gain for a Q-wire with a width of 15 nm and for a Q-film structure was calculated at 300 K. The thickness in the growth direction is 7 nm for the Q-wire and Q-film structures. As can be seen in Fig. 4, the maximum gain and differential gain are markedly reduced with increasing size distribution ($\Delta W/W_0$). In the case of $\Delta W/W_0 = 40\%$, the maximum gain and differential gain of the Q-wire structure are inferior to those of the Q-film structure. Accordingly, to observe strong lateral confinement for Q-wires, a size distribution of less than 10% ($\Delta W/W_0 < 10\%$) is necessary.

C. Strain Effect in Q-Wires

Q-wires fabricated by etching and regrowth produce a strain effect. The strain distribution in such Q-wires is calculated using an analytical technique based on a 2-D Green's function for the stress field. An eight-band $k{\cdot}p$ theory was used for calculating the energy band structures including strain relaxation. The experimentally observed wire-width dependence of the large energy blue shift in the PL spectrum of partially strain-compensated (SC) GaInAsP/InP vertically stacked multiple Q-wires can be accurately plotted without using any fitting parameter [84].

D. Polarization Anisotropy of Q-Wires

The in-plane polarization anisotropy of optical gain in compressively strained (CS) GaInAsP/InP Q-wire lasers including elastic-strain-relaxation-induced band mixing has been studied [85]. Fig. 5 shows the maximum material gain as a function of carrier density N for a 10-nm-wide SC-SQW Q-wire. The maximum possible gain is obtained at the $E_{//}$ polarization. We also observed that the transparent carrier density N_g in the $E_{//}$

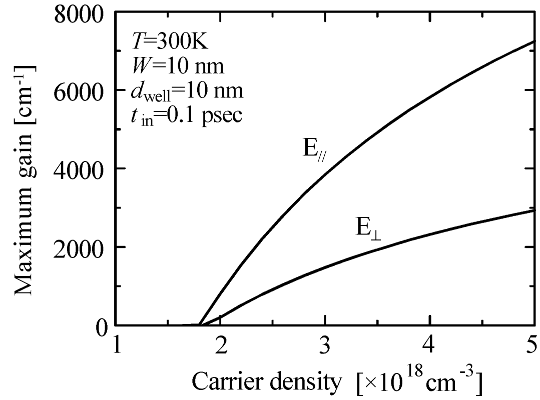

Fig. 5. Injection carrier density dependence of maximum gain of the SC-SQW for $E_{//}$ and $E_{\perp}$.

polarization is smaller than that in the $E_{\perp}$ polarization, where $E_{//}$ represents the parallel polarization along the wire direction and $E_{\perp}$ the normal polarization perpendicular to the wire direction.

E. Recombination Velocity at Eched/Regrown Interface

The carrier lifetime ($\tau_{\rm s}$), incorporating additional nonradiative recombination processes from the sidewalls of the active region via the surface recombination velocity (S), can be expressed as follows [86], [87]:

$$\frac{1}{\tau_{\rm s}} \cong B_{\rm eff} N + \frac{2S}{W - 2W_{\rm d}} \tag{3}$$

where W is the wire width, $B_{\rm eff}$ is the effective recombination coefficient, N is the carrier density, and $W_{\rm d}$ is the so-called "dead layer" width, and is regarded as a region that does not generate photoexcited carriers [88].

F. Threshold Current

The equation of threshold current density ($J_{\rm th}$) can be rewritten as

$$J_{\rm th} = \frac{edN_w \rho N_{\rm th}}{\tau_{\rm s}} \tag{4}$$

where e is the electronic charge, d is the thickness of one active layer, N_w is the number of active layers, ρ is the in-plane space filling factor of the active regions ($\rho = W/\Lambda$), and $N_{\rm th}$ is the threshold carrier density.

The dependence of the relative threshold current density [$J_{\rm th}$(Q-wire)/$J_{\rm th}$(Q-film)] on S was calculated at 300 K, as shown in Fig. 6. To ensure that the change in the threshold current density is less than 10% of the case for $S = 0$ cm/s ($S = 0$ implies no nonradiative recombination at the etched/regrown interfaces), S should be smaller than 30 cm/s.

IV. Fabrication Processes and Optical Properties of Quantum Structures by Dry Etching and Regrowth

A. Fabrication Process

Fig. 7 shows the fabrication process for Q-wire lasers. An SC-5QW structure was prepared on a (1 0 0) p+-InP substrate

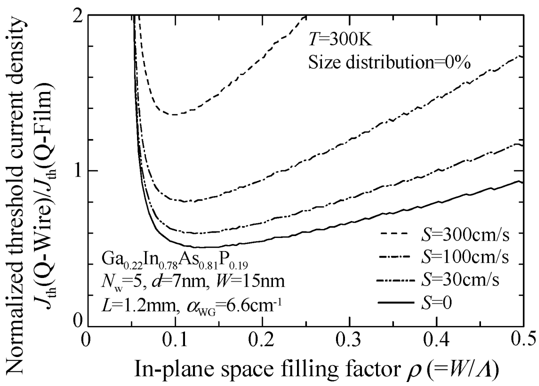

Fig. 6. In-plane space filling factor (ρ) dependence of the relative threshold current density. The surface recombination velocity (S) is 0, 30, 100, and 300 cm/s.

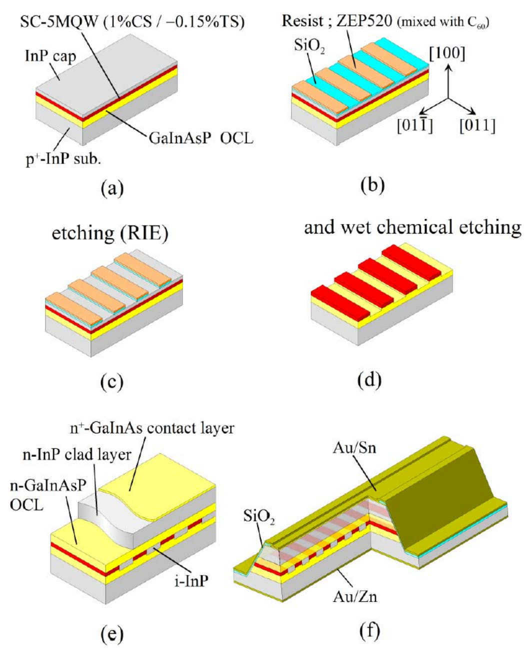

Fig. 7. Fabrication process of Q-wire structure by dry etching and regrowth for Q-wire laser. (a) 1st OMVPE. (b) SiO_2 CVD and EB lithography. (c) CF_4 reative ion etching (RIE). (d) CH_4/H_2-RIF and wet chemical etching. (e) 2nd OMVPE. (f) Mesa stripe laser.

as an initial wafer by OMVPE growth. The introduction of the SC-QW structure consisting of CS wells and TS barrier layers is very effective for the reduction of nonradiative recombination at etched/regrown interfaces and the suppression of 3-D stress due to a large lattice mismatch along the vertical structure between CS wells and unstrained barrier layers induced during etching and InP embedding regrowth [89], [90]. The initial wafer comprises a p-InP buffer layer, an undoped $Ga_{0.22}In_{0.78}As_{0.47}P_{0.53}$ optical confinement layer (OCL), five $Ga_{0.22}In_{0.78}As_{0.81}P_{0.19}$ 1% CS-QW layers sandwiched by six -0.15% TS barrier layers, a GaInAsP OCL layer, and an InP cap layer [see Fig. 7(a)]. After the deposition of a 20-nm-thick SiO_2 layer on the wafer, a Q-wire pattern parallel to the [0 1 1] direction and perpendicular to the direction of the cavity was described by EB lithography using ZEP520 resist mixed with C_{60}

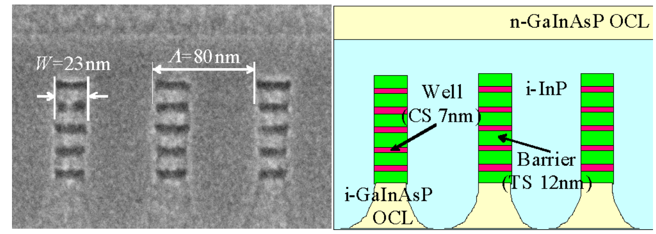

Fig. 8. Cross-sectional SEM view of Q-wire23.

microcomposite [see Fig. 7(b)]. Then, the EB pattern was transferred to the SiO_2 layer by CF_4-RIE [see Fig. 7(c)]. Using the 20-nm-thick SiO_2 mask, active layers were completely etched by CH_4/H_2-RIE [see Fig. 7(d)]. CH_4/H_2-RIE and O_2 ashing steps were repeated several times throughout the etching to remove the polymer deposited during RIE and acquire a vertical shape. To remove layers damaged by the dry etching process, a small amount of wet chemical etching was carried out before the regrowth. After removing the SiO_2 mask using BHF, the regrowth was carried out by the OMVPE technique [see Fig. 7(e)]. First, i-InP was grown into the groove regions at 600 °C at a slow growth speed (250 nm/h) [69]. Then, an n-GaInAsP OCL layer, an n-InP cladding layer, and an n+-GaInAs contact layer were grown at 650 °C at a growth speed of 1.2 μm/h. Fig. 8 shows a cross-sectional SEM view around the Q-wire active region and its schematic diagram. The typical wire width was measured to be 23 nm, which corresponds to $\rho = W/\Lambda = 0.29$.

B. Size Distributions and Interface Quality of Q-Wires

The size distributions of the Q-wire structures were measured by SEM views, and the standard deviation was estimated to be less than ±2 nm. From the Q-film EL spectra at 103 K, the full-width at half-maximum of these Q-wire structures was comparable to that of the Q-film structure fabricated from the same initial QW [91].

The product of the surface recombination velocity at the etched/regrown interfaces and the carrier lifetime was estimated from the relative spontaneous emission efficiency of the Q-wire structure $\eta_{\mathrm{spon,Wire}}$ normalized by that of the initial Q-film structure $\eta_{\mathrm{spon,Film}}$, as expressed in (3). As a consequence, the product $S \cdot \tau_s$ was less than 3 nm [92], which corresponds to $S = 100$ cm/s for $\tau_s = 3$ ns. These results indicate the low damage to the etched/regrown interface of the GaInAsP/InP Q-wire structure fabricated by dry etching and regrowth with the SC-QW structure as the initial wafer.

C. Arbitrary-Shaped Low-Dimensional Quantum Structure

Arbitrary-shaped quantum structures such as Q-wires with width of 6–39 nm [93], Q-wires with lengths of 60–1000 nm [94], and Q-dot and L-shaped quantum structures [95] can be realized with better dimensional and positional controllability using the improved process.

The polarization anisotropy of these quantum structures was also observed through the lateral quantum confinement effect [96].

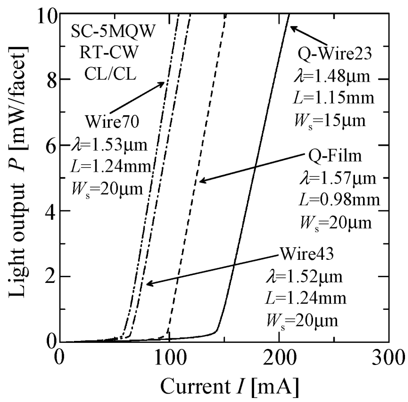

Fig. 9. L–I characteristics of Q-wire23, wire43, wire70, and Q-film lasers under RT-CW conditions.

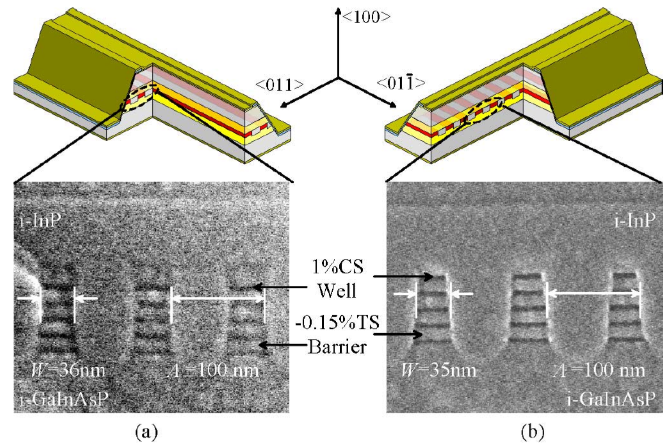

Fig. 10. Schematic diagram and cross-sectional SEM view. (a) Q-wire$_{//}$ laser. (b) Q-wire$_{\perp}$ laser.

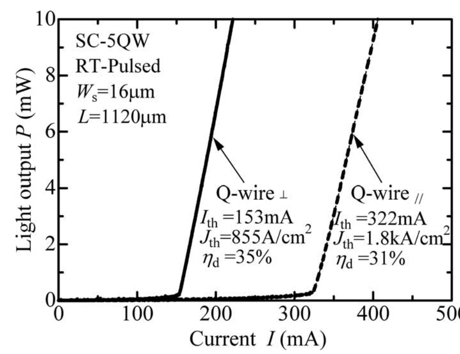

Fig. 11. L–I characteristics of Q-wire$_{//}$ and Q-wire$_{\perp}$ lasers under RT-pulsed condition.

V. Long-Wavelength Q-Wire Lasers

The GaInAsP/InP Q-wire lasers fabricated by dry etching and regrowth were operated at RT under pulse [95], [97] and CW operations [98]. Fig. 9 shows the light output characteristics under RT-CW conditions for Q-wire23 (wire width of 23 nm), wire43 (wire width of 43 nm), a wire-like laser (wire width of 70 nm in a period of 120 nm, wire70, for short), and a Q-film laser fabricated from the same initial QW structure.

Operation at a low-threshold current density due to the volume effect of the active region was observed in wire43 and wire70, but the threshold current density of Q-wire23 was higher than that of the Q-film laser and its differential quantum efficiency was slightly lower than that of the others, probably due to the oscillation from the first excited levels with a too small volume of the active region for the given cavity design.

The reliable RT-CW operation of Q-wire lasers was obtained without any serious performance degradation even after 40 000 h [Reliable operation over 7000 h was reported in ref. [102]; the same device is still operating].

A. *Polarization Anisotropy of Optical Gain*

To observe the polarization anisotropy of optical gain against the wire direction, two types of Q-wire lasers were fabricated simultaneously by the aforementioned method where the Q-wire structures were arranged parallel (Q-wire$_{//}$) and perpendicular (Q-wire$_{\perp}$) to the cavity direction. Fig. 10 shows a schematic diagram of both Q-wire lasers. Both Q-wire lasers had a uniform wire width of 35 nm.

Fig. 11 shows the light output characteristics of Q-wire$_{//}$ and Q-wire$_{\perp}$ lasers under a pulsed condition (1 μs width, 1 kHz repetition) at RT. The cavity length (L) and stripe width (W_s) of these lasers were 1120 and 16 μm, respectively. As shown in Fig. 11, the threshold current density of the Q-wire$_{//}$ (1.8 kA/cm^2) laser was approximately 2.1 times higher than that of the Q-wire$_{\perp}$ laser (855 A/cm^2). Such a difference should originate from either a different function of Q-wire structures or different cavity characteristics, as explained next.

The origins of this anomalous threshold current may be due to three important parameters in the lasing conditions: 1) the difference in total optical loss in the devices; 2) the difference in active volume; and 3) the differences in differential gain and transparency carrier density.

The total optical loss in the laser cavity can be simply expressed as the sum of waveguide loss and mirror loss. However, the waveguide loss and mirror loss are considered as constant parameters became the laser cavity length and cleavage mirror facets were used in the measurements. The quality of the Q-wire structure interfaces and waveguide loss should not have a significant effect for such different threshold conditions.

The similar wire widths of Q-wire$_{//}$ and Q-wire$_{\perp}$ were confirmed by SEM images, as shown in Fig. 10. The size distribution in both Q-wire lasers was almost the same according to the spontaneous emission spectra at 2% of the threshold current, and should not affect the lasing conditions. As a result, the difference in active volume is not the reason for these anomalous threshold currents.

According to the aforementioned experimental results, the total optical loss and active volume cannot be significant reasons for the large difference in threshold current of the Q-wire$_{//}$ and Q-wire$_{\perp}$ lasers. The relationship between the differential gain and the transparent carrier density is thus the most probable cause of this phenomenon. The differential gain can be obtained from the plot of the peak material gain of the Q-wire structures.

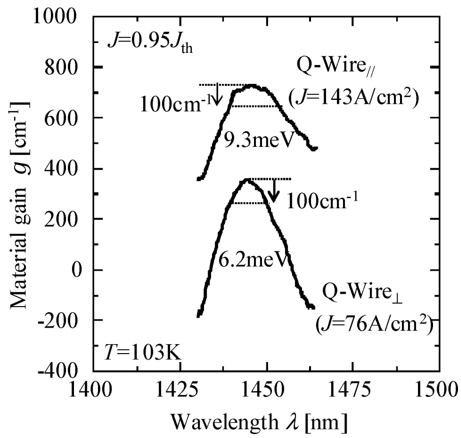

Fig. 12. Material gain spectra of Q-wire$_{//}$ and ~~Q-wire~~ lasers under CW condition below threshold ($I = 0.95 I_{\mathrm{th}}$) at 103 K. Q-wir

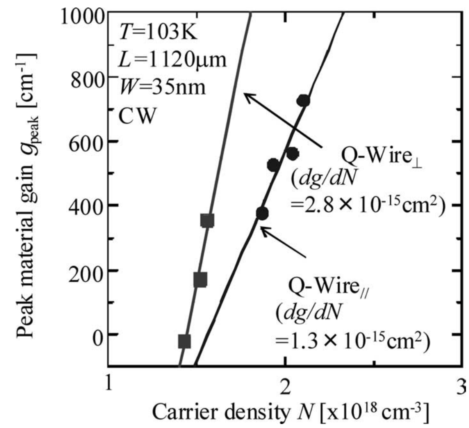

Fig. 13. ~~Material gain spectra of Q-wire$_{//}$ and Q-wire$_{\perp}$ lasers under CW condition below threshold ($I = 0.95 I_{\mathrm{th}}$) at 103 K.~~

Peak material gain of Q-wire// and Q-wire^ la

In this experiment, Hakki–Paoli's method was utilized to determine the material gain spectra [99].

The optical gain spectra were measured at 103 K because it was necessary to measure the material gain under the CW condition. Fig. 12 shows the material gain spectra of both Q-wire lasers. The spectral width at 100 cm^{-1} below the peak for the Q-wire$_{\perp}$ laser (6.2 meV) was narrower than that for the Q-wire$_{//}$ laser (9.3 meV). The broadening of the material gain spectral width of the Q-wire$_{//}$ laser has not been experimentally reported elsewhere. It may be caused by not only the higher injection carrier density, but also the anisotropic property of the transition matrix element due to the lateral quantum confinement effect in the Q-wire structure that was observed in the calculated result for Q-wire structure grown on V-grooved substrate [100]. The anisotropic differential gain in Q-wire$_{//}$ and Q-wire$_{\perp}$ lasers is an important parameter for evaluating the anisotropy of their threshold currents. The material gain spectra of both Q-wire$_{//}$ and Q-wire$_{\perp}$ lasers were measured at various injection current densities varying from 75% to 95% of the threshold level for each Q-wire laser.

Fig. 13 shows the measured peak material gain as a function of the injection carrier density. The same threshold gain can be observed in both Q-wire lasers. From the least-squares fitting method, the differential gain was obtained to be 1.3×10^{-15} and 2.8×10^{-15} cm^2 for the Q-wire$_{//}$ and Q-wire$_{\perp}$ lasers, respectively. The Q-wire$_{\perp}$ laser has a differential gain approximately 2.2 times higher than that of the Q-wire$_{//}$ laser. A slight difference in the transparent carrier density of these Q-wire lasers was also observed. This might be caused by inaccurate linear curve fitting near the transparent carrier density level. Nevertheless, its magnitude should not have much effect on such anisotropic lasing characteristics. Conversely, the estimated threshold current density of the Q-wire$_{//}$ laser is estimated to be 1.7 times higher than that of the Q-wire$_{\perp}$ laser by using the estimated value of differential optical gain that is in agreement with the experimental result (J_{th} : Q-wire$_{//} = 1.8 \times J_{\mathrm{th}}$: Q-wire$_{\perp}$). These results clearly show that the anomalous lasing characteristics of Q-wire$_{//}$ and Q-wire$_{\perp}$ lasers are caused by the anisotropic differential gain in Q-wire structures that contributes to their polarization dependence of the dipole moment. However, this anisotropy was stronger than that theoretically predicted [100]. It is considered that the 2-D elastic strain relaxation effect in the strained Q-wire might have enhanced the quantum confinement effect similar to the enhancement of energy blue shift in the strained Q-wire [84], [101].

B. *Q-Wire DBR Lasers*

GaInAsP/InP multiple-layered Q-wire lasers with an SiO_2/semiconductor DBR were realized for low-threshold lasing [102]. Oscillations due to the transition between the ground levels were obtained at RT. In addition, the threshold current densities of these Q-wire lasers were lower than that of Q-film lasers. The differential quantum efficiency of these Q-wire lasers was also comparable to that of Q-film lasers.

C. *Q-Wire DFB Lasers*

Q-wire DFB lasers with a low-threshold current and high differential quantum efficiency were successfully realized under RT-CW condition [103], [104]. Fig. 14 shows a cross-sectional SEM view of the Q-wire DFB active region. The spontaneous emission efficiency of this Q-wire DFB laser was comparable to that of a Q-film laser fabricated by one-step growth. A single-mode operation with an SMSR of 50 dB at a bias current of twice the threshold current was also achieved.

A single-mode operation with high characteristic temperature was achieved for 1590 nm GaInAsP/InP Q-wire DFB lasers by adopting Bragg wavelength detuning from the gain peak wavelength [105]. Single-mode operation and a characteristic temperature of 95 K were obtained over a temperature range of 20 °C to 80 °C, as shown in Fig. 15. These results indicate that Bragg wavelength detuning with a Q-wire DFB laser is very attractive for temperature-insensitive and low-threshold-current operation [106].

D. *High-Performance Lasers Using Q-Wire Passive Section*

We proposed a new integration method utilizing the energy blue shift observed in Q-wire lasers. This energy blue shift

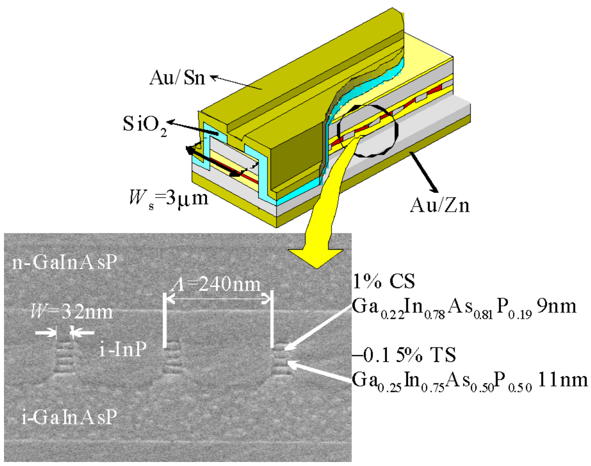

Fig. 14. Cross-sectional SEM view of the Q-wire DFB laser.

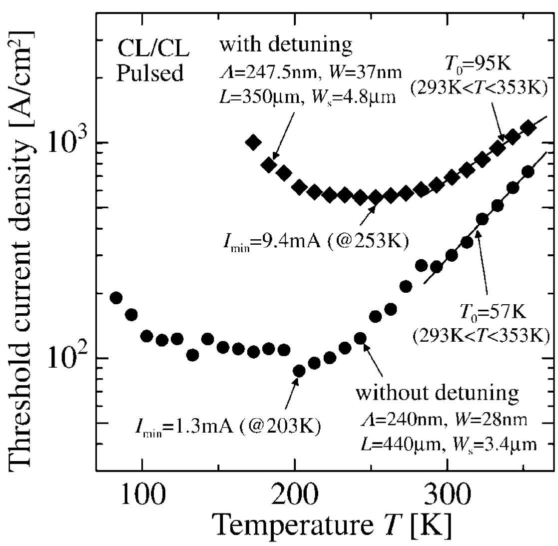

Fig. 15. Temperature dependence of L–I characteristics of Q-wire DFB lasers.

can be applied for the integration of various types of photonic devices. A blue shift of over 30 meV was obtained for the wire widths of less than 30 nm [84].

The emission wavelength can be controlled by adjusting the wire width. An emission wavelength of 1.55 μm can be used for the gain regions, such as lasers and amplifiers. Using shorter wavelengths, namely, in the case of narrower wires, modulators and switches can be realized. Longer wavelengths can be applied to detectors. Therefore, the integration of various types of photonic devices is expected by modulating wire widths in the same wafer [107]. This integration technique utilizing the energy blue shift is advantageous for realizing the high-density integration of various elements with the same crystal quality in the active and passive sections.

A distributed reflector (DR) laser, which consists of active DFB and passive DBR sections, was proposed, and low-threshold and high-efficiency operations were realized [108]. A novel DR laser, which is one of the applications of the integration method utilizing the lateral quantum confinement effect, was

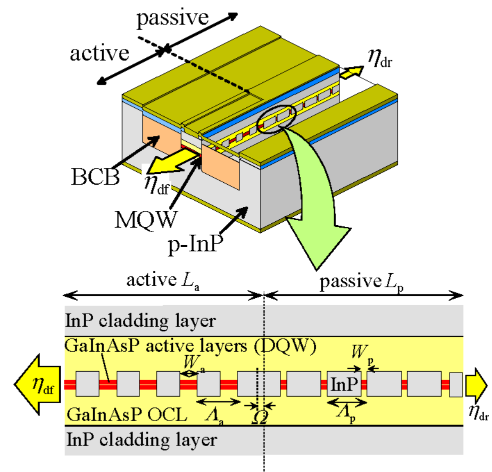

Fig. 16. Schematic structure of DR laser.

proposed [109], and a low-threshold-current, high-efficiency, stable single-mode operation was realized [110], [111].

Fig. 16 shows the schematic structure of the new type of DR laser, which consists of an active DFB section with periodically etched wire-like active regions and a passive DBR section with a narrow Q-wire structure. To realize high reflectivity, a low-loss waveguide is necessary. Thus, the transition energy in the DBR section was enhanced by utilizing the energy blue shift due to the lateral quantum confinement effect by using narrower wires. Recently, the threshold current of as low as 0.8 mA was obtained by utilizing a deep DFB grating region in the active section for higher index coupling coefficient [112].

The monolithic integration of a DR laser with a front power monitor utilizing a narrow Q-wire structure has been realized [113]. The front power monitor is a new concept; a low-absorption waveguide section is placed in front of an active or another passive device to monitor the modulated signal power. It can be used at any position in photonic ICs with minimum interference from the signal.

VI. Conclusion

Recent progress in the research on long-wavelength GaInAsP/InP Q-wire lasers is reviewed. Although there still remain problems to be solved for a realization of high-performance lasers required for the fabrication of low-dimensional structures, we can demonstrate moderately good size uniformity and low damage to the etched/regrown interface of GaInAsP/InP strain-compensated multiple-layered Q-wire structures fabricated by EB lithography, CH_4/H_2-RIE, and two-step OMVPE growth. Arbitrary-shaped quantum structures were also realized by this method. It was found that the anisotropic optical gain in the Q-wire structure is the reason for the anomalous characteristics in Q-wire lasers. As an approach to reducing the threshold current density, we introduced DBR and DFB structures in the cavity and realized the low-threshold-current RT-CW operation of Q-wire lasers. In the present stage, the threshold current of Q-wire lasers is worse than that of Q-film lasers. The reason is that the narrow gain spectrum caused by the quantum confinement effect cannot be obtained by size fluctuation in Q-wire structure fabricated by our method. To reduce the size fluctuation, low-temperature development [114], nanoimprinting lithography [115], block copolymer lithography [116], [117], etc., are proposed.

In addition, low-threshold current and high differential quantum efficiency with stable single-mode operations were achieved for DR lasers that are composed of wire-like active regions with a DFB cavity and a passive DBR region with Q-wire structures.

Therefore, these results indicate that this fabrication method is very promising for the realization of not only high-performance lasers but also various photonic devices consisting of arbitrary-shaped low-dimensional structures with high position controllability.

ACKNOWLEDGMENT

The authors would like to thank Prof. E. Y. Suematsu, Prof. E. K. Iga, Prof. K. Kobayashi, Prof. K. Furuya, Prof. M. Asada, and Prof. F. Koyama, and Associate Professors Y. Miyamoto, M. Watanabe, T. Miyamoto, H. Uenohara, and N. Nishiyama of Tokyo Institute of Technology for fruitful discussions. They also acknowledge all of former/present students who have been involved in the investigations of low-damage fabrication processes of ultrafine structures for GaInAsP/InP long-wavelength quantum wire lasers and related photonic devices in our group from mid-1980s.

REFERENCES

[1] N. Holonyak, Jr., R. M. Kolbas, R. D. Dupuis, and P. D. Dapkus, "Quantum-well heterostructure lasers," *IEEE J. Quantum Electron.*, vol. QE-16, no. 2, pp. 170–186, Feb. 1980.

[2] A. R. Adams, "Band-structure engineering for low-threshold high-efficiency semiconductor lasers," *Electron. Lett.*, vol. 22, no. 5, pp. 249–250, Feb. 1986.

[3] E. Yablonovitch and E. O. Kane, "Reduction of lasing threshold current density by the lowering of valence band effective mass," *J. Lightw. Technol.*, vol. JLT-4, no. 5, pp. 504–506, May 1986.

[4] P. J. A. Thijs, L. F. Tiemeijer, P. I. Kindersma, J. J. M. Binsma, and T. Van Dongen, "High-performance 1.5 μm wavelength InGaAs-InGaAsP strained quantum well lasers and amplifiers," *IEEE J. Quantum Electron.*, vol. 27, no. 6, pp. 1426–1439, Jun. 1991.

[5] Y. Arakawa and H. Sakaki, "Multidimensional quantum well laser and temperature dependence of its threshold current," *Appl. Phys. Lett.*, vol. 40, no. 11, pp. 939–941, Jun. 1982.

[6] M. Asada, Y. Miyamoto, and Y. Suematsu, "Gain and the threshold of three-dimensional quantum-box lasers," *IEEE J. Quantum Electron.*, vol. QE-22, no. 9, pp. 1915–1921, Sep. 1986.

[7] C. Henry, "Theory of the linewidth of semiconductor lasers," *IEEE J. Quantum Electron.*, vol. QE-18, no. 2, pp. 259–264, Feb. 1982.

[8] Y. Miyake and M. Asada, "Spectral characteristics of linewidth enhancement factor α of multidimensional quantum wells," *Jpn. J. Appl. Phys.*, vol. 28, no. 7, pp. 1280–1281, Jul. 1989.

[9] Y. Arakawa and A. Yariv, "Quantum well lasers—gain, spectra, dynamics," *IEEE J. Quantum Electron.*, vol. 22, no. 9, pp. 1887–1899, Sep. 1986.

[10] S. Ueno, Y. Miyake, and M. Asada, "Advantage of strained quantum wire lasers," *Jpn. J. Appl. Phys.*, vol. 31, no. 2A, pp. 286–287, Feb. 1992.

[11] K. J. Vahala, "Quantum box fabrication tolerance and size limits in semiconductors and their effect on optical gain," *IEEE J. Quantum Electron.*, vol. QE-24, no. 3, pp. 523–530, Mar. 1988.

[12] H. Zarem, K. Vahala, and A. Yariv, "Gain spectra of quantum wires with inhomogeneous broadening," *IEEE J. Quantum Electron.*, vol. 25, no. 4, pp. 705–712, Apr. 1989.

[13] P. M. Petroff, A. C. Gossard, R. A. Logan, and W. Wiegmann, "Toward quantum well wires: Fabrication and optical properties," *Appl. Phys. Lett.*, vol. 41, no. 7, pp. 635–638, Oct. 1982.

[14] E. Inamura, Y. Miyamoto, S. Tamura, T. Takasugi, and K. Furuya, "Wet chemical etching for ultrafine periodic structure: Rectangular InP corrugations of 70 nm pitch and 100 nm depth," *Jpn. J. Appl. Phys.*, vol. 28, no. 10, pp. 2193–2196, Oct. 1989.

[15] K. G. Ravikumar, K. Kudo, S. Arai, and Y. Suematsu, "Low-damage GaInAs(P)/InP nanometer structure by low-pressure ECR-RIBE," *Jpn. J. Appl. Phys.*, vol. 29, no. 10, pp. L1744–L1746, Oct. 1990.

[16] K. Kudo, Y. Nagashima, M. Tamura, S. Tamura, A. Ubukata, and S. Arai, "Fabrication of GaInAs/GaInAsP/InP multi-quantum-wires and -boxes by substrate-potential-controlled electron cyclotron resonance reactive ion beam etching," *Jpn. J. Appl. Phys.*, vol. 33, no. 10A, pp. L1382–L1385, Oct. 1994.

[17] T. Yamamoto, E. Inamura, Y. Miyamoto, and K. Furuya, "OMVPE buried ultrafine periodic structures in GaInAs and InP," *Microelectron. Eng.*, vol. 11, pp. 93–96, Apr. 1990.

[18] M. Notomi, M. Naganuma, T. Nishida, T. Tamamura, H. Iwamura, S. Nojima, and M. Okamoto, "Clear energy level shift in ultranarrow InGaAs/InP quantum well wires fabricated by reverse mesa chemical etching," *Appl. Phys. Lett.*, vol. 58, no. 7, pp. 720–722, Feb. 1991.

[19] S. Wakabayashi, Y. Toyoda, H. Tougou, T. Narusawa, Y. Nagamune, and Y. Arakawa, "Fabrication of AlGaAs/GaAs multi-QWRs with 15 nm wire width using two-step etching and MBE regrowth," in *Nanostructures and Quantum Effects,* vol. 31 (Springer Series in Materials Sciences), H. Sakaki and H. Noge, Eds. Heidelberg, Germany: Springer-Verlag, 1994, pp. 194–196.

[20] B. Hübner, B. Jacobs, C. Greus, R. Zengerle, and A. Forchel, "Luminescence spectroscopy of dry etched single dots and wires," *J. Vac. Sci. Technol.*, vol. B12, no. 6, pp. 3658–3662, Nov./Dec. 1994.

[21] K. Moriyasu, S. Osako, N. Mori, and C. Hamaguchi, "Effect of quantum confinement and lattice relaxation on electronic states in $\mathrm{GaAs/In_{0.2}Ga_{0.8}As/GaAs}$ quantum dots," *Jpn. J. Appl. Phys.*, vol. 36, no. 6B, pp. 3932–3935, Jun. 1997.

[22] Y. S. Tang, C. D. W. Wilkinson, D. W. Smith, T. E. Whall, and E. H. C. Parker, "Optical properties of dry-etched $\mathrm{Si/Si_{1-x}Ge_x}$ heterostructure wires," *Jpn. J. Appl. Phys.*, vol. 33, no. 4B, pp. 2348–2352, Apr. 1994.

[23] T. Takizawa, S. Arai, and M. Nakahara, "Fabrication of vertical and uniform-size porous InP structure by electrochemical anodization," *Jpn. J. Appl. Phys.*, vol. 33, no. 5A, pp. L643–L645, May 1994.

[24] S. Y. Chou, P. R. Krauss, W. Zhang, L. Guo, and L. Zhuang, "Sub-10 nm impact lithography and applications," *J. Vac. Sci. Technol. B, Microelectron. Process. Phenom.*, vol. 15, no. 6, pp. 2897–2904, Nov./Dec. 1997.

[25] M. Tsuchiya, J. M. Gaines, R. H. Yan, R. J. Simes, P. O. Holtz, L. A. Coldren, and P. M. Petroff, "Optical anisotropy in a quantum-well-wire array with two-dimensional quantum confinement," *Phys. Rev. Lett.*, vol. 62, no. 4, pp. 466–469, Jan. 1989.

[26] M. Kitamura, M. Nishioka, J. Oshinowo, and Y. Arakawa, "Formation of InGaAs quantum dots on GaAs multi-atomic steps by metalorganic chemical vapor deposition growth," *Jpn. J. Appl. Phys.*, vol. 34, no. 8B, pp. 4376–4379, Aug. 1995.

[27] S. Hara, J. Motohisa, T. Fukui, and H. Hasegawa, "Quantum well wire fabrication method using self-organized multiatomic steps on vicinal (0 0 1) GaAs surfaces by metalorganic vapor phase epitaxy," *Jpn. J. Appl. Phys.*, vol. 34, no. 8B, pp. 4401–4404, Aug. 1995.

[28] M. Higashiwaki, M. Yamamoto, T. Higuchi, S. Shimomura, A. Adachi, Y. Okamoto, N. Sano, and S. Hiyamizu, "High-density GaAs/AlAs quantum wires grown on (775)B-oriented GaAs substrates by molecular beam epitaxy," *Jpn. J. Appl. Phys.*, vol. 35, no. 5B, pp. L606–L608, May 1996.

[29] S. Hara, J. Motohisa, and T. Fukui, "Formation and characterization of InGaAs strained quantum wires on GaAs multiatomic steps grown by metalorganic vapor phase epitaxy," *J. Cryst. Growth*, vol. 170, pp. 579–584, Jan. 1997.

[30] T. Kato, T. Takeuchi, Y. Inoue, S. Hasegawa, K. Inoue, and H. Nakashima, "Stacked GaAs multi-quantum wires grown on vicinal GaAs(1 1 0) surfaces by molecular beam epitaxy," *Appl. Phys. Lett.*, vol. 72, no. 4, pp. 465–467, Jan. 1998.

[31] S. Tsukamoto, Y. Nagamune, M. Nishioka, and Y. Arakawa, "Fabrication of GaAs arrowhead-shaped quantum wires by metalorganic chemical vapor deposition selective growth," *Appl. Phys. Lett.*, vol. 62, no. 1, pp. 49–51, Jan. 1993.

[32] I. Matsuyama, M. Lopez, N. Tanaka, and T. Ishikawa, "Cathodoluminescence of wirelike GaAs/AlAs quantum well structures grown on substrate patterned with [0 0 1] mesa stripes," *Jpn. J. Appl. Phys.*, vol. 33, no. 5A, pp. L627–L630, May 1994.

[33] T. Sogawa, S. Ando, and H. Kanbe, "Lateral-size control of trench-buried quantum wires using GaAs/AlAs superlattice layers," *Jpn. J. Appl. Phys.*, vol. 34, no. 8B, pp. 4405–4407, Aug. 1995.

[34] N. Hatori, T. Mukaihara, Y. Hayashi, N. Ohnoki, F. Koyama, and K. Iga, "Design and fabrication of InGaAs/GaAs quantum wires for vertical-cavity surface emitting lasers," *Jpn. J. Appl. Phys.*, vol. 35, no. 3, pp. 1777–1778, Mar. 1996.

[35] H. Weman, M.-A. Dupertuis, E. Martinet, A. Rudra, and E. Kapon, "Efficient, narrow linewidth excitonic emission at room temperature from GaAs/AlGaAs V-groove quantum wire light-emitting diodes," *Appl. Phys. Lett.*, vol. 79, no. 1, pp. 4–6, Jul. 2001.

[36] M. Araki, Y. Hanada, H. Fujikura, and H. Hasegawa, "Fabrication of InGaAs quantum wires and dots by selective molecular beam epitaxy growth on various mesa-patterned (0 0 1)InP substrates," *Jpn. J. Appl. Phys.*, vol. 36, no. 3B, pp. 1763–1769, Mar. 1997.

[37] M. Kappelt, M. Grundmann, A. Krost, V. Türck, and D. Bimberg, "InGaAs quantum wires grown on by low pressure metalorganic chemical vapor deposition on InP V-grooves," *Appl. Phys. Lett.*, vol. 68, no. 25, pp. 3596–3598, Jun. 1996.

[38] C. A. C. Mendonca, E. Laureto, M. J. S. P. Brasil, M. A. Cotta, M. M. G. Carvalho, and E. A. Meneses, "On the optical properties of InAs/InP systems: The role of two-dimensional structures and three-dimensional islands," *Appl. Phys. Lett.*, vol. 72, no. 9, pp. 1015–1017, Feb. 1998.

[39] K. Komori, A. Hamano, S. Arai, Y. Miyamoto, and Y. Suematsu, "Fabrication of GaInAs/InP quantum wires by organometallic-vapor-phase-epitaxial (OMVPE) selective growth on grooved side walls of ultrafine multilayers," *Jpn. J. Appl. Phys.*, vol. 31, no. 5A, pp. L535–L538, May 1992.

[40] W. Wegscheider, L. N. Pfeiffer, A. Pinczuk, K. W. West, M. M. Dignam, R. Hull, and R. E. Leibenguth, "GaAs/AlGaAs quantum wire lasers fabricated by cleaved edge overgrowth," *J. Cryst. Growth*, vol. 150, pp. 285–292, May 1995.

[41] M. Takeuchi, K. Shiba, K. Sato, H. K. Huang, K. Inoue, and H. Nakashima, "Formation and characterization of GaAs quantum wires at giant step edges on vicinal (1 1 0) GaAs surfaces," *Jpn. J. Appl. Phys.*, vol. 34, no. 8B, pp. 4411–4413, Aug. 1995.

[42] N. Tomita, M. Tanaka, T. Saeki, S. Shimomura, S. Hiyamizu, K. Fujita, T. Watanabe, T. Higuchi, N. Sano, and A. Adachi, "Improved cathodluminescence properties of GaAs/Al0.3Ga0.7As tilted T-shaped quantum wires fabricated on (1 1 1)B facet by glancing-angle molecular beam epitaxy," *J. Vac. Sci. Technol. B, Microelectron. Process. Phenom.*, vol. 14, no. 6, pp. 3550–3554, Nov./Dec. 1996.

[43] K. C. Hsieh, J. N. Baillargeon, and K. Y. Cheng, "Compositional modulation and long-range ordering in GaP/InP short-period superlattices grown by gas source molecular beam epitaxy," *Appl. Phys. Lett.*, vol. 57, no. 19, pp. 2244–2246, Nov. 1990.

[44] K. Y. Cheng, K. C. Hsieh, and J. N. Baillargeon, "Formation of lateral quantum wells in vertical short-period superlattices by strain-induced lateral-layer ordering process," *Appl. Phys. Lett.*, vol. 60, no. 23, pp. 2892–2894, Jun. 1992.

[45] S. Francoeur, A. G. Norman, A. Mascarenhas, E. D. Jones, J. L. Reno, S. R. Lee, and D. M. Follstaedt, "Two-dimensional array of self-assembled AlInAs quantum wires," *Appl. Phys. Lett.*, vol. 81, no. 3, pp. 529–531, Jan. 1998.

[46] N. N. Ledentsov, "Self-organized quantum wires and dots: New challenge for device applications," presented at the Int. Conf. EW MOVPE VII, Berlin, Germany, Jun. 1997.

[47] M. Tsuchiya, P. M. Petroff, and L. A. Coldren, "Use of tilted-superlattices for quantum-well-wire lasers," *IEEE Trans. Electron Devices*, vol. 36, no. 11, pp. 2612–2613, Nov. 1989.

[48] M. Higashiwaki, S. Shimomura, and S. Hiyamizu, "Self-organized GaAs quantum-wire lasers grown on (7 7 5) B-oriented GaAs substrates by molecular beam epitaxy," *Appl. Phys. Lett.*, vol. 74, no. 6, pp. 780–782, Feb. 1999.

[49] Y. Miyamoto, M. Cao, Y. Shingai, K. Furuya, Y. Suematsu, K. G. Ravikumar, and S. Arai, "Light emission from quantum-box structure by current injection," *Jpn. J. Appl. Phys.*, vol. 26, no. 4, pp. L225–L227, Apr. 1987.

[50] P. Daste, Y. Miyake, M. Cao, Y. Miyamoto, S. Arai, Y. Suematsu, and K. Furuya, "Fabrication technique for GaInAsP/InP quantum wire structure by LP-MOVPE," *J. Cryst. Growth*, vol. 93, pp. 365–369, Nov./Dec. 1988.

[51] D. Gershoni, H. Temkin, G. J. Dolan, J. Dunsmuir, S. N. G. Chu, and M. B. Panish, "Effects of two-dimensional confinement on the optical properties of InGaAs/InP quantum wire structures," *Appl. Phys. Lett.*, vol. 53, no. 11, pp. 995–997, Sep. 1988.

[52] M. Cao, Y. Miyake, S. Tamura, H. Hirayama, S. Arai, Y. Suematsu, and Y. Miyamoto, "Lasing action in GaInAs/GaInAsP quantum-wire structure," *Trans. IEICE*, vol. E73, no. 1, pp. 63–70, Jan. 1990.

[53] E. Kapon, S. Simhony, R. Bhat, and D. M. Hwang, "Single quantum wire semiconductor lasers," *Appl. Phys. Lett.*, vol. 55, no. 25, pp. 2715–2717, Dec. 1989.

[54] S. Tiwari, G. D. Pettit, K. R. Milkove, F. Legoues, R. J. Davis, and J. M. Woodall, "High efficiency and low threshold current strained V-groove quantum-wire lasers," *Appl. Phys. Lett.*, vol. 64, no. 26, pp. 3536–3538, Jun. 1994.

[55] T. G. Kim, X.-L. Wang, Y. Suzuki, K. Komori, and M. Ogura, "Characteristics of the ground-state lasing operation in V-groove quantum-wire lasers," *IEEE J. Sel. Topics Quantum Electron.*, vol. 6, no. 3, pp. 511–521, May/Jun. 2000.

[56] S. T. Chou, K. Y. Cheng, L. J. Chou, and K. C. Hsieh, "$\mathrm{Ga}_x\mathrm{In}_{1-x}$ multiple-quantum-wire lasers grown by the strain-induced lateral-layer ordering process," *Appl. Phys. Lett.*, vol. 66, no. 17, pp. 2220–2222, Apr. 1995.

[57] U. A. Griesinger, H. Schweizer, V. Härle, J. Hommel, F. Barth, B. Höhing, B. Klepser, and F. Scholz, "Dry-etched wire distributed feedback laser," *IEEE Photon. Technol. Lett.*, vol. 7, no. 9, pp. 953–955, Sep. 1995.

[58] N. Nunoya, M. Nakamura, H. Yasumoto, S. Tamura, and S. Arai, "GaInAsP/InP multiple-layered quantum-wire lasers fabricated by CH_4/H_2 reactive-ion etching," *Jpn. J. Appl. Phys.*, vol. 39, no. 6A, pp. 3410–3415, Jun. 2000.

[59] N. Nunoya, M. Nakamura, M. Morshed, S. Tamura, and S. Arai, "High-performance 1.55 μm wavelength GaInAsP/InP distributed feedback lasers with wirelike active regions," *IEEE J. Sel. Topics Quantum Electron.*, vol. 7, no. 2, pp. 249–258, Mar./Apr. 2001.

[60] K. Kudo, Y. Nagashima, S. Tamura, S. Arai, Y. Huang, and Y. Suematsu, "$\mathrm{Ga}_{0.66}\mathrm{In}_{0.34}\mathrm{As/GaInAsP/InP}$ tensile-strained single-quantum-well lasers with 70-nm period wire active region," *IEEE Photon. Technol. Lett.*, vol. 5, no. 8, pp. 864–867, Aug. 1993.

[61] K. C. Shin, S. Arai, Y. Nagashima, K. Kudo, and S. Tamura, "Temperature dependences of $\mathrm{Ga}_{0.66}\mathrm{In}_{0.34}\mathrm{As\text{-}InP}$ tensile-strained quasi-quantum-wire laser fabricated by wet chemical etching and 2-step OMVPE growth," *IEEE Photon. Technol. Lett.*, vol. 7, no. 4, pp. 345–347, Apr. 1995.

[62] T. Kojima, M. Tamura, H. Nakaya, S. Tanaka, S. Tamura, and S. Arai, "GaInAsP/InP compressively strained quantum-wire lasers fabricated by electron beam lithography and 2-step organometallic vapor phase epitaxy," *Jpn. J. Appl. Phys.*, vol. 37, no. 9A, pp. 4792–4800, Sep. 1998.

[63] T. Kojima, H. Nakaya, S. Tanaka, H. Yasumoto, S. Tamura, and S. Arai, "Temperature dependence of internal quantum efficiency of 20 nm-wide GaInAsP/InP compressively strained quantum-wire lasers," *Jpn. J. Appl. Phys.*, vol. 38, no. 1B, pp. 585–588, Jan. 1999.

[64] M. B. Stern, H. G. Craighead, P. F. Liao, and P. M. Mankiewich, "Fabrication of 20-nm structures in GaAs," *Appl. Phys. Lett.*, vol. 45, no. 4, pp. 410–412, Aug. 1984.

[65] J.-N. Patillon, C. Jay, C. Delallande, M. Iost, J.-P. Andre, H. L. Coz, M. Signles-Frehel, O. Vlaeminck, and V. Soucail, "New dry etching method for the fabrication of InP/InGaAs quantum wires," *Jpn. J. Appl. Phys.*, vol. 30, no. 2B, pp. L252–L254, Feb. 1991.

[66] H. Kitada, H. Arimoto, A. Tackeuchi, Y. Yamaguchi, Y. Nakata, A. Endoh, and S. Muto, "Fabrication of sub-100 nm wires and dots in GaAs/AlGaAs multiquantum well using focused ion beam lithography," *Jpn. J. Appl. Phys.*, vol. 31, no. 7B, pp. L990–L991, Jul. 1992.

[67] J. Hommel, M. Moser, M. Geiger, F. Scholz, and H. Schweizer, "Investigations of dry etching in AlGaInP/GaInP using CCl_2F_2/Ar reactive ion etching and Ar ion beam etching," *J. Vac. Sci. Technol.*, vol. B9, no. 6, pp. 3526–3529, Nov./Dec. 1991.

[68] N. Nunoya, M. Nakamura, H. Yasumoto, S. Tamura, and S. Arai, "Low threshold GaInAsP/InP distributed feedback lasers with periodic wire active regions fabricated by CH_4/H_2 reactive ion etching," *Jpn. J. Appl. Phys.*, vol. 38, no. 11B, pp. L1323–L1326, Nov. 1999.

[69] A. Talneau, N. Bouadma, Y. Lebellego, S. Slempkes, A. Ougazzaden, G. Patriarche, and B. Sermage, "Low-damage dry-etched grating on an MQW active layer and dislocation-free InP regrowth for 1.55-μm complex-coupled DFB lasers fabrication," *IEEE Photon. Technol. Lett.*, vol. 10, no. 8, pp. 1070–1072, Aug. 1998.

[70] G. T. Liu, A. Stintz, H. Li, T. C. Newell, A. L. Gray, P. M. Varangis, K. J. Malloy, and L. F. Lester, "The influence of quantum-well composition on the performance of quantum dot lasers using InAs/InGaAs

dots-in-a-well (DWELL) structures," *IEEE J. Quantum Electron.*, vol. 36, no. 11, pp. 1272–1279, Nov. 2000.
[71] K. Mukai, Y. Nakata, K. Otsubo, M. Sugawara, N. Yokoyama, and H. Ishikawa, "1.3 μm CW lasing characteristics of self-assembled InGaAs-GaAs quantum dots," *IEEE J. Quantum Electron.*, vol. 36, no. 4, pp. 472–478, Apr. 2000.
[72] F. Klopf, R. Krebs, A. Wolf, M. Emmerling, J. P. Reithmaier, and A. Forchel, "InAs/GaInAs quantum dot DFB lasers emitting at 1.3 μm," *Electron. Lett.*, vol. 37, no. 10, pp. 634–636, May 2001.
[73] Z. Mi, P. Bhattacharya, and J. Yang, "Growth and characteristics of ultralow threshold 1.45 μm metamorphic InAs tunnel injection quantum dot lasers on GaAs," *Appl. Phys. Lett.*, vol. 89, no. 15, pp. 153109-1–153109-3, Oct. 2006.
[74] H. Saito, K. Nishi, and S. Sugou, "Ground-state lasing at room temperature in long-wavelength InAs quantum-dot lasers on InP(311)B substrates," *Appl. Phys. Lett.*, vol. 78, no. 3, pp. 267–269, Jan. 2001.
[75] R. H. Wang, A. Stintz, P. M. Varangis, T. C. Newell, H. Li, K. J. Malloy, and L. F. Lester, "Room-temperature operation of InAs quantum-dash lasers on InP(001)," *IEEE Photon. Technol. Lett.*, vol. 13, no. 8, pp. 767–769, Aug. 2001.
[76] E. Homeyer, R. Piron, F. Grillot, O. Dehaese, K. Tavernier, E. Macé, J. Even, A. L. Corre, and S. Loualiche, "Demonstration of a low threshold current in 1.54 μm InAs/InP(3 1 1)B quantum dot laser with reduced quantum dot stacks," *Jpn. J. Appl. Phys.*, vol. 46, no. 10A, pp. 6903–6905, Oct. 2007.
[77] D. Piester, P. Bönsch, T. Schrimpf, H.-H. Wehmann, and A. Schlachetzki, "Laser-action in V-groove-shaped InGaAs-InP single quantum wires," *IEEE J. Sel. Topics Quantum Electron.*, vol. 6, no. 3, pp. 522–526, May/Jun. 2000.
[78] P. J. A. Thijs, J. J. M. Binsma, L. F. Tiemeijer, and T. Van Dongen, "Submilliamp threshold current (0.62 mA at 0 °C) and high output power (220 mW) 1.5 μm tensile strained InGaAs single quantum-well lasers," *Electron. Lett.*, vol. 28, no. 9, pp. 829–830, Apr. 1992.
[79] G. T. Liu, A. Stintz, H. Li, K. J. Malloy, and L. F. Lester, "Extremely low room-temperature threshold current density diode lasers using lnAs dots in $\mathrm{In_{0.5}Ga_{0.85}As}$ quantum well," *Electron. Lett.*, vol. 35, no. 14, pp. 1163–1165, Jul. 1999.
[80] M. Asada and Y. Suematsu, "Density-matrix theory of semiconductor lasers with relaxation broadening model—Gain and gain-suppression in semiconductor lasers," *IEEE J. Quantum Electron.*, vol. QE-21, no. 5, pp. 434–442, May 1985.
[81] M. Asada, A. Kameyama, and Y. Suematsu, "Gain and intervalence band absorption in quantum-well lasers," *IEEE J. Quantum Electron.*, vol. QE-20, no. 7, pp. 745–753, Jul. 1984.
[82] M. Asada, Y. Miyamoto, and Y. Suematsu, "Theoretical gain of quantum-well wire lasers," *Jpn. J. Appl. Phys.*, vol. 24, no. 2, pp. L95–L97, Feb. 1985.
[83] M. Yamada, H. Ishiguro, and H. Nagato, "Estimation of the intra-band relaxation time in undoped AlGaAs injection laser," *Jpn. J. Appl. Phys.*, vol. 19, no. 1, pp. 135–142, Jan. 1980.
[84] A. Haque, H. Yagi, T. Sano, T. Maruyama, and S. Arai, "Electronic band structures of GaInAsP/InP vertically stacked multiple quantum wires with strain-compensating barriers," *J. Appl. Phys.*, vol. 94, no. 3, pp. 2018–2023, Aug. 2003.
[85] A. Haque, T. Maruyama, H. Yagi, T. Sano, D. Plumwongrot, and S. Arai, "Anomalous in-plane polarization dependence of optical gain in compressively strained GaInAsP/InP quantum wire lasers," *IEEE J. Quantum Electron.*, vol. 40, no. 9, pp. 1344–1351, Sep. 2004.
[86] B. E. Maile, A. Forchel, and R. Germann, "Impact of sidewall recombination on the quantum efficiency of dry etched InGaAs/InP semiconductor wires," *Appl. Phys. Lett.*, vol. 54, no. 16, pp. 1552–1554, Apr. 1989.
[87] M. Tamura, T. Kojima, T. Ando, N. Nunoya, S. Tamura, and S. Arai, "Sidewall recombination velocity in GaInAsP/InP quantum-well lasers with wire-like active region fabricated by wet-chemical etching and organo-metallic vapor-phase-epitaxial regrowth," *Jpn. J. Appl. Phys.*, vol. 37, no. 12A, pp. 6569–6574, Dec. 1998.
[88] M. Tamura, T. Ando, N. Nunoya, S. Tamura, S. Arai, and G. Bacher, "Estimation of sidewall nonradiative recombination in GaInAsP/InP wire structure fabricated by low energy electro-cyclotron-resonance reactive-ion-beam-etching," *Jpn. J. Appl. Phys.*, vol. 37, no. 6A, pp. 3576–3584, Jun. 1998.
[89] N. Nunoya, H. Yasumoto, H. Midorikawa, S. Tamura, and S. Arai, "Low threshold current density operation of GaInAsP/InP lasers with strain-compensated multiple-layered wirelike active regions," *Jpn. J. Appl. Phys.*, vol. 39, no. 10B, pp. L1042–1045, Oct. 2000.
[90] H. Yagi, K. Muranushi, N. Nunoya, T. Sano, S. Tamura, and S. Arai, "Low-damage etched/regrown interface of strain-compensated GaInAsP/InP quantum-wire laser fabricated by $\mathrm{CH_4/H_2}$ dry etching and regrowth," *Appl. Phys. Lett.*, vol. 81, no. 6, pp. 966–968, Aug. 2002.
[91] T. Sano, H. Yagi, K. Muranushi, S. Tamura, T. Maruyama, A. Haque, and S. Arai, "Multiple-quantum-wire structures with good size uniformity fabricated by $\mathrm{CH_4/H_2}$ dry etching and organometallic vapor-phase-epitaxial regrowth," *Jpn. J. Appl. Phys.*, vol. 42, no. 6A, pp. 3471–3472, Jun. 2003.
[92] H. Yagi, T. Sano, K. Ohira, D. Plumwongrot, T. Maruyama, A. Haque, S. Tamura, and S. Arai, "GaInAsP/InP partially strain-compensated multiple-quantum-wire lasers fabricated by dry etching and regrowth processes," *Jpn. J. Appl. Phys.*, vol. 43, no. 6A, pp. 3401–3409, Jun. 2004.
[93] H. Itoh, M. Yoshita, H. Akiyama, D. Plumwongrot, T. Maruyama, and S. Arai, "Micro-photoluminescence characterizations of GaInAsP/InP single quantum wires fabricated by dry etching and regrowth," *J. Appl. Phys.*, vol. 102, no. 9, pp. 093509-1–093509-5, Nov. 2007.
[94] D. Plumwongrot, Y. Tamura, Y. Nishimoto, M. Kurokawa, T. Maruyama, N. Nishiyama, and S. Arai, "Length dependencies of in-plane polarizations anisotropy in GaInAsP/InP quantum-wire structures fabricated by dry etching and regrowth process," presented at the OPTO2008 (part of SPIE Photon. West 2008), San Jose, CA, Jan.
[95] D. Plumwongrot, Y. Tamura, T. Maruyama, N. Nishiyama, and S. Arai, "Fabrication of GaInAsP/InP arbitrary shaped low dimensional quantum structures," in *Proc. 20th Int. Microprocess. Nanotechnol. Conf. (MNC 2007)*, Kyoto, Japan, Nov. 2007, pp. 156–157.
[96] D. Plumwongrot, T. Maruyama, A. Haque, H. Yagi, K. Miura, Y. Nishimoto, and S. Arai, "Polarization anisotropy of spontaneous emission spectra in GaInAsP/InP quantum-wire structures," *Jpn. J. Appl. Phys.*, vol. 47, no. 5, pp. 3735–3741, May 2008.
[97] H. Yagi, K. Muranushi, N. Nunoya, T. Sano, S. Tamura, and S. Arai, "GaInAsP/InP strain-compensated quantum-wire lasers fabricated by CH_4/H_2 dry etching and organometallic vapor-phase-epitaxial regrowth," *Jpn. J. Appl. Phys.*, vol. 41, no. 2B, pp. L186–L189, Feb. 2002.
[98] H. Yagi, T. Sano, K. Ohira, T. Maruyama, A. Haque, and S. Arai, "Room temperature-continuous wave operation of GaInAsP/InP multiple-quantum-wire lasers by dry etching and regrowth method," *Jpn. J. Appl. Phys.*, vol. 42, no. 7A, pp. L748–L750, Jul. 2003.
[99] W. Hakki and T. L. Paoli, "Gain spectra in GaAs double-heterostructure injection lasers," *J. Appl. Phys.*, vol. 46, no. 3, pp. 1299–1306, Mar. 1975.
[100] D. M. Gvozdic, N. M. Nenadovic, and A. Schlachetzki, "Gain and threshold-current calculation of V-groove quantum-wire InGaAs-InP laser," *IEEE J. Quantum Electron.*, vol. 38, no. 12, pp. 1565–1579, Dec. 2002.
[101] M. Notomi, J. Hammersberg, J. Zeman, H. Weman, M. Potemski, H. Sugiura, and T. Tamamura, "Polarization and broken symmetry due to anisotropic "triaxial" strain states in lattice-mismatched quantum wires," *Phys. Rev. Lett.*, vol. 14, no. 14, pp. 3125–3128, Apr. 1998.
[102] H. Yagi, T. Sano, K. Miura, D. Plumwongrot, K. Ohira, T. Maruyama, and S. Arai, "GaInAsP/InP long-wavelength lasers with strain-compensated quantum-wire active regions and $\mathrm{SiO_2}$/semiconductor reflectors," *IEICE Electron. Exp.*, vol. 1, no. 17, pp. 540–544, Dec. 2004.
[103] H. Yagi, K. Miura, Y. Nishimoto, D. Plumwongrot, K. Ohira, T. Maruyama, and S. Arai, "Low-threshold-current operation of 1540 nm GaInAsP/InP distributed-feedback lasers with multiple-quantum-wire active regions," *Appl. Phys. Lett.*, vol. 87, no. 22, pp. 223120-1–223120-3, Nov. 2005.
[104] Y. Nishimoto, K. Miura, H. Yagi, D. Plumwongrot, K. Ohira, T. Maruyama, and S. Arai, "Low-threshold current density GaInAsP/InP quantum-wire distributed feedback lasers fabricated by low-damage processes," *Jpn. J. Appl. Phys.*, vol. 46, no. 2, pp. L34–L36, Feb. 2007.
[105] Y. Nishimoto, H. Yagi, K. Miura, D. Plumwongrot, K. Ohira, T. Maruyama, and S. Arai, "High T_0 operation of 1590 nm GaInAsP/InP quantum-wire distributed feedback lasers by Bragg wavelength detuning," *Jpn. J. Appl. Phys.*, vol. 46, no. 17, pp. L411–L413, Apr. 2007.
[106] D. Plumwongrot, Y. Nishimoto, S. M. Ullah, Y. Tamura, M. Kurokawa, T. Maruyama, N. Nishiyama, and S. Arai, "Bragg wavelength detuning in GaInAsP/InP DFB lasers with wirelike active regions," *Jpn. J. Appl. Phys.*, vol. 46, no. 45, pp. L1090–L1092, Nov. 2007.
[107] S. Arai, H. Yagi, K. Ohira, T. Maruyama, and S. Tamura, "GaInAsP/InP quantum-wire lasers and distributed reflector lasers with wirelike active

regions by lithography and regrowth," *Proc. SPIE, Novel In-Plane Semicond. Lasers IV*, vol. 5738, pp. 303–317, Apr. 2005.

[108] J.-I. Shim, K. Komori, S. Arai, I. Arima, Y. Suematsu, and R. Somchai, "Lasing characteristics of 1.5 μm GaInAsP-InP SCH-BIG-DR lasers," *IEEE J. Quantum. Electron.*, vol. 27, no. 6, pp. 1736–1745, Jun. 1991.

[109] K. Ohira, T. Murayama, H. Yagi, S. Tamura, and S. Arai, "Low-threshold distributed reflector laser consisting of wide and narrow wirelike active regions," *IEEE Photon. Technol. Lett.*, vol. 17, no. 2, pp. 264–266, Feb. 2005.

[110] K. Ohira, T. Murayama, S. M. Ullah, H. Yagi, and S. Arai, "GaInAsP/InP distributed reflector laser with phase-shifted DFB and quantum-wire DBR sections," *IEICE Electron. Exp.*, vol. 2, no. 11, pp. 356–361, Jun. 2005.

[111] K. Ohira, T. Murayama, S. Tamura, and S. Arai, "Low-threshold and high-efficiency operation of distributed reflector lasers with width-modulated wirelike active regions," *IEEE J. Sel. Topics Quantum Electron.*, vol. 11, no. 5, pp. 1162–1168, Sep./Oct. 2005.

[112] S. M. Ullah, R. Suemitsu, S. Lee, M. Otake, N. Nishiyama, and S. Arai, "Low-threshold-current operation of high-mesa stripe distributed reflector laser emitting at 1540 nm," *Jpn. J. Appl. Phys.*, vol. 46, no. 44, pp. L1068–L1070, Nov. 2007.

[113] S. Lee, R. Suemitsu, S. M. Ullah, M. Otake, N. Nishiyama, and S. Arai, "Very high electric isolation resistance between distributed reflector laser and front power monitor through deeply etched narrow groove," *Jpn. J. Appl. Phys.*, vol. 46, no. 39, pp. L954–L956, Oct. 2007.

[114] L. E. Ocola and A. Stein, "Effect of cold development on improvement in electron-beam nanopatterning resolution and line roughness," *J. Vac. Sci. Technol. B, Microelectron. Process. Phenom.*, vol. 22, no. 4, pp. 1711–1716, Jul./Aug. 2004.

[115] Y. Kurashima, H. Hiroshima, M. Komuro, S.-H. Kim, N. Yamazaki, J. Taniguchi, I. Miyamoto, H. Namatsu, and S. Matsui, "Fabrication of low line edge roughness mold for photo-nanoimprint," *Jpn. J. Appl. Phys.*, vol. 43, no. 6B, pp. 4045–4049, Jun. 2004.

[116] M. Park, C. Harrison, P. M. Chaikin, R. A. Register, and D. H. Adamson, "Block copolymer lithography: Periodic arrays of $\sim 10^{11}$ holes in 1 square centimeter," *Science*, vol. 276, no. 5317, pp. 1401–1404, May 1997.

[117] I. Bita, J. K. W. Yang, Y. S. Jung, C. A. Ross, E. L. Thomas, and K. K. Berggren, "Graphoepitaxy of self-assembled block copolymers on two-dimensional periodic patterned templates," *Science*, vol. 321, no. 5891, pp. 939–943, Aug. 2008.

Shigehisa Arai (M'83–SM'06) was born in Kanagawa, Japan, in 1953. He received the B.E., M.E., and D.E. degrees in electronics from Tokyo Institute of Technology, Tokyo, Japan, in 1977, 1979, and 1982, respectively.

In 1982, he was a Research Associate in the Department of Physical Electronics, Tokyo Institute of Technology, where he became an Associate Professor in 1987 and a Professor at the Research Center for Quantum Effect Electronics in 1994. From 1983 to 1984, he was with AT&T Bell Laboratories, Holmdel, NJ. Since 2004, he has been a Professor with the Quantum Nanoelectronics Research Center, Tokyo Institute of Technology. His current research interests include photonic integrated devices, such as dynamic-single-mode and wavelength-tunable semiconductor lasers, semiconductor optical amplifiers, and optical switches/modulators. He is also involved in research of low-damage and cost-effective processing technologies of ultrafine structures for high-performance lasers and photonic integrated circuits on a silicon platform.

Prof. Arai is a member of the Optical Society of America, the Institute of Electronics, Information and Communication Engineers (IEICE), and the Japan Society of Applied Physics (JSAP). He received an Excellent Paper Award from the IEICE of Japan in 1988, the Michael Lunn Memorial Award from the Indium Phosphide and Related Materials Conference in 2000, Prizes for science and technology including a Commendation for Science and Technology from the Minister of Education, Culture, Sports, Science and Technology in 2008, an Electronics Society Award from IEICE in 2008, and a JSAP Fellowship in 2008.

Takeo Maruyama (M'08) was born in Toyama, Japan, in 1972. He received the B.E. degree in electrical and electronic engineering, and the M.E. and Ph.D. degrees in physical electronics from Tokyo Institute of Technology, Tokyo, Japan, in 1997, 1999, and 2002, respectively.

In 2002, he was a Research Associate at the Research Center for Quantum Effect Electronics, Tokyo Institute of Technology, where he was engaged in research on the development of semiconductor membrane lasers on silicon substrates based on direct bonding. Since 2008, he has been with the School of Electrical and Computer Engineering, Kanazawa University, Ishikawa, Japan. His current research interests include photonic integrated devices on a silicon platform.

Dr. Maruyama is a member of the Japan Society of Applied Physics and the Institute of Electronics, Information and Communication Engineers of Japan. He received the Hiroshi Ando Memorial Young Engineer Award from The Foundation of Ando Laboratory.